Article

Copper Oxide Nanocrystals

Ming Yin, Chun-Kwei Wu, Yongbing Lou, Clemens Burda,
Jeffrey T. Koberstein, Yimei Zhu, and Stephen O'Brien

J. Am. Chem. Soc., **2005**, 127 (26), 9506-9511• DOI: 10.1021/ja050006u • Publication Date (Web): 10 June 2005

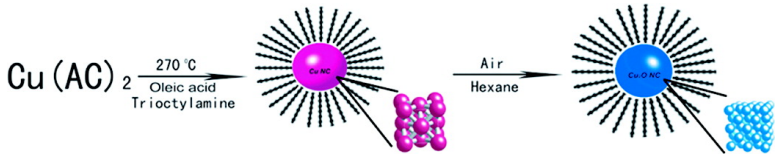

More About This Article

Additional resources and features associated with this article are available within the HTML version:

- Supporting Information
- Links to the 27 articles that cite this article, as of the time of this article download
- Access to high resolution figures
- Links to articles and content related to this article
- Copyright permission to reproduce figures and/or text from this article

View the Full Text HTML

J|A|C|S
ARTICLES
Published on Web 06/10/2005

Copper Oxide Nanocrystals

Ming Yin,[†] Chun-Kwei Wu,[‡] Yongbing Lou,[§] Clemens Burda,[§] Jeffrey T. Koberstein,[‡] Yimei Zhu,[⊥] and Stephen O'Brien*,[†]

Contribution from the Department of Applied Physics and Applied Mathematics and Department of Chemical Engineering, Materials Research Science and Engineering Center, Columbia University, New York, New York 10027, Department of Chemistry, Center for Chemical Dynamics and Nanomaterials Research, Case Western Reserve University, Cleveland, Ohio 44106, and Department of Materials Science, Brookhaven National Lab, Upton, New York 11973

Received January 2, 2005; E-mail: so188@columbia.edu

Abstract: It is well-known that inorganic nanocrystals are a benchmark model for nanotechnology, given that the tunability of optical properties and the stabilization of specific phases are uniquely possible at the nanoscale. Copper (I) oxide (Cu_2O) is a metal oxide semiconductor with promising applications in solar energy conversion and catalysis. To understand the $Cu/Cu_2O/CuO$ system at the nanoscale, we have developed a method for preparing highly uniform monodisperse nanocrystals of Cu_2O. The procedure also serves to demonstrate our development of a generalized method for the synthesis of transition metal oxide nanocrystals. Cu nanocrystals are initially formed and subsequently oxidized to form highly crystalline Cu_2O. The volume change during phase transformation can induce crystal twinning. Absorption in the visible region of the spectrum gave evidence for the presence of a thin, epitaxial layer of CuO, which is blue-shifted, and appears to increase in energy as a function of decreasing particle size. XPS confirmed the thin layer of CuO, calculated to have a thickness of ~5 Å. We note that the copper (I) oxide phase is surprisingly well-stabilized at this length scale.

Introduction

Copper (I) oxide (Cu_2O) is a *p*-type metal oxide semiconductor with promising applications in solar energy conversion and catalysis.[1−4] There has been much interest in Cu_2O (also called cuprous oxide) due to its electronic structure. The large excitonic binding energy (140 meV) allows the observation of a well-defined series of excitonic features in the absorption and luminescence spectrum at low temperature,[5,6] yet studying quantum confinement effects or modifying the behavior of the direct forbidden band gap is very challenging,[7,8] It is also an ideal compound to study the influence of electron-correlation effects on the electronic structure of transition metal compounds in general, and the high T_c superconductors in particular.[2] Although the absorption characteristics of the various exciton series for copper (I) oxide have been studied.[5,9−13] Most samples have been limited to bulk, μm-sized particles or nanopowders. In addition, Rockenberger et al. reported a single precursor decomposition approach to nanoparticles of iron and copper oxides.[14] We have established a procedure by which discrete, monodisperse, and uniform nanocrystals of pure copper are extracted from solution that can be completely oxidized to Cu_2O. Cu_2O is a prospective candidate for low-cost photovoltaic applications due to its high optical absorption coefficient, lower band gap energy (2.2 eV), and simplicity of preparation, scalability, the nontoxic nature, the abundance, and the economics of the material. Further opportunities in catalysis could be realized through the preparation of self-assembled nanostructures and stabilization of specific phases of copper oxide. Therefore, it is of fundamental interest to prepare high-quality, monodisperse copper oxide nanocrystals to examine their structure and characterize their optical properties. An investigation and understanding of size effects in such a system is also of interest due to the possibility of tuning its optoelectronic properties. Substantial effort has been devoted to the $Cu/Cu_2O/CuO$ system

[†] Department of Applied Physics and Applied Mathematics.
[‡] Department of Chemical Engineering, Materials Research Science and Engineering Center, Columbia University.
[§] Case Western Reserve University.
[⊥] Brookhaven National Lab.

(1) Dong, Y.; Li, Y.; Wang, C.; Cui, A.; Deng, Z. *J. Colloid. Interface Sci.* **2001**, *243*, 85.
(2) Ram, S.; Mitra, C. *Mater. Sci. Eng.* **2001**, *A304−306*, 805.
(3) Musa, A. O.; Akomolafe, T.; Carter, M. J. *Sol. Energy Mater. Sol. Cells* **1998**, *51*, 305.
(4) Bohannan, E. W.; Shumsky, M. G.; Switzer, J. A. *Chem. Mater.* **1999**, *11*, 2289.
(5) Deki, S.; Akamatsu, K.; Yano, T.; Mizuhata, M.; Kajinami, A. *J. Mater. Chem.* **1998**, *8*, 1865.
(6) Caswell, N.; Yu, P. Y. *Phys. Rev. B* **1982**, *25*, 5519.
(7) Borgohain, K.; Murase, N.; Mahamuni, S. *J. Appl. Phys.* **2002**, *92*, 1292.
(8) Amikura, H.; Masumi, T. *J. Phys. Soc. Jpn.* **1995**, *64*, 2684.
(9) Trebin, H. R.; Cummins, H. Z.; Birman, J. L. *Phys. Rev. B* **1981**, *23*, 597.
(10) Gastev, S. V.; Kaplyanskii, A. A.; Sokolov, N. S. *Solid State Commun.* **1982**, *42*, 389.
(11) Snoke, D. W.; Wolfe, J. P.; Mysyrowicz, A. *Phys. Rev. B* **1990**, *41*, 11171.
(12) Snoke, D. W.; Braun, D.; Cardona, M. *Phys. Rev. B* **1991**, *44*, 2991.
(13) Goto, T.; Shen, M. Y.; Koyama, S.; Yokouchi, T. *Phys. Rev. B* **1997**, *55*, 7609.
(14) Rockenberger, J.; Scher, E. C.; Alivisatos, A. P. *J. Am. Chem. Soc.* **1999**, *121*, 11595.

 10.1021/ja050006u CCC: $30.25

in the 1−500-nanometer range.[15−19] Our approach involves thermal decomposition of copper (I) acetate at high temperature, in the presence of a surfactant. The result is highly monodispersed and crystalline nanoparticles of Cu_2O, with a mean particle size tunable from 3.6 ± 0.8 to 10.7 ± 0.7 nm (based upon the stoichiometric ratio of surfactant to copper precursor). Evidence of Cu^{2+} in the XPS and optical characterization of the nanocrystals suggested the existence of a thin layer of CuO at the nanocrystal−ligand interface.

Crystals of a finite size may assume a modified morphology and/or crystal structure so that the atoms, especially those at the surface, can adopt the most stable equilibrium configuration of minimal energy.[2] Consequently, some materials, which are not stable in the bulk and do not exist in ambient atmosphere, may become substantially more stable at the nanoscale. This is largely due to the large contribution of surface energy which can stabilize the origin of unique phases.[20−22] Nanoscale Cu_2O is observed to be relatively stable with respect to bulk Cu_2O, which can readily convert to CuO in air at room temperature.[2] The reason for this morphological and stoichiometric control is still a subject of discussion in the literature, although crystal structure is believed to play a part.[23]

Experimental Section

Nanocrystal Synthesis. Copper (I) acetate (CH_3CO_2Cu), trioctylamine ($[CH_3(CH_2)_7]_3N$), oleic acid ($CH_3(CH_2)_7CH{=}CH(CH_2)_7CO_2H$), hexane, and ethanol were purchased from Aldrich and used as received. In a typical synthesis, a solution containing 4 mmol copper acetate, 4 mL of oleic acid, and 15 mL of trioctylamine was quickly heated to 180 °C. Under nitrogen, the color gradually changed from forest green to coffee, finally producing a gray colloid. The presence of oxygen or water is highly undesirable during the decomposition and nucleation stage. The solution was kept at this temperature for 1 h and then quickly heated to 270 °C. The gray colloid gradually changed to a deep burgundy solution. The solution was kept at 270 °C for an hour before it was cooled to room temperature, and particles were precipitated by ethanol and redispersed in hexane. The particles (Cu) are observed to be initially dark red, forming a purple/dark-red solution when dispersed in hexane. The resulting red purple copper particles gradually oxidize to Cu_2O in hexane, and produce a deep green solution. The final Cu_2O nanocrystals were very stable in hexane, both with respect to oxidation and agglomeration, and ready to be used for further experiments.

TEM and XRD Characterization. Cu_2O nanocrystals were characterized using transmission electron microscopy (JEOL CX100) with an accelerating voltage of 100 kV, high-resolution TEM (JEOL 3000F) with an accelerating voltage of 300 kV, and X-ray powder diffraction (Scintag X_2 X-ray diffractometer). TEM samples were prepared by placing a drop of a dilute hexane dispersion of nanocrystals on the surface of a 400-mesh copper grid backed with Formvar and were dried in a vacuum chamber for 1 h. JEOL 3000F was used for lattice imaging. XRD samples were prepared by drying a dispersion of nanocrystals on a piece of Si (100) wafer (Figure 1).

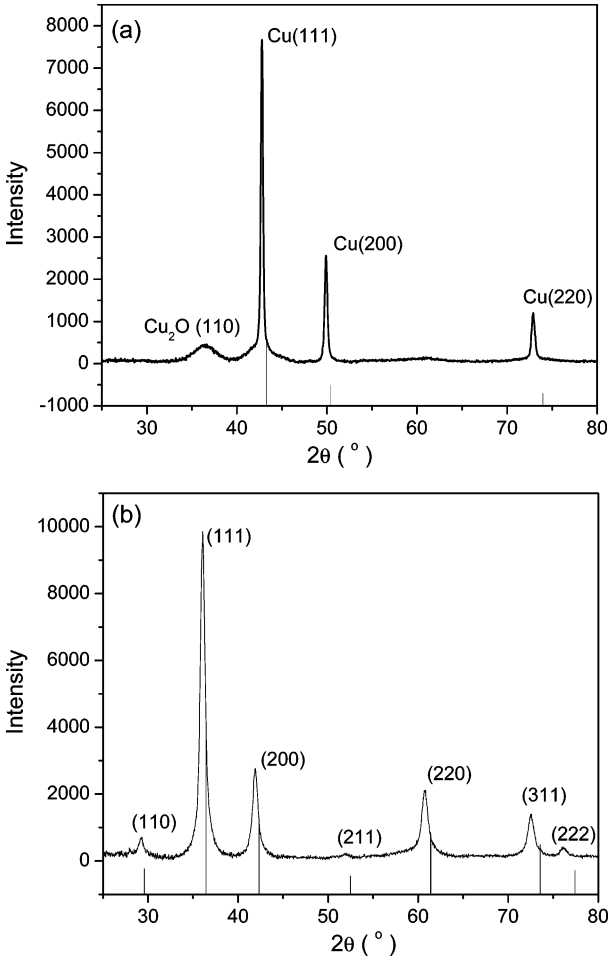

Figure 1. (a) X-ray powder diffraction patterns of fcc Cu nanocrystals, 10 min after synthesis and extraction from solution. (b) X-ray powder diffraction patterns of 5-nm cuprite Cu_2O nanocrystals, sample prepared after oxidation.

UV−Vis Characterization. The UV−vis absorbance and fluorescence spectra were measured on a Varian Cary 50 and a Varian Eclipse fluorescence spectrophotometer, respectively. XPS characterization. The XPS experiment was performed on PHI 5500 model spectrometer equipped with an Al Kα monochromator X-ray source running at 15 kV, a hemispherical electron energy analyzer, and a multichannel detector. The test chamber pressure was maintained below 2×10^{-9} Torr during spectral acquisition. A low-energy electron flood gun was used to neutralize the possible surface charge. The XPS binding energy (BE) was internally referenced to the aliphatic C(1s) peak (BE, 284.6 eV). Survey spectra were acquired at an analyzer pass energy of 93.9 eV, while high-resolution spectra were acquired with a pass energy of 23.5 eV. The takeoff angle is defined as the angle between the surface normal and detector. High-resolution spectra were resolved by fitting each peak with Guassian−Lorentz functions after subtracting the background using the PHI data processing software package under the constraint of setting a reasonable BE shift and characteristic full width at half-maximum range. Atomic concentrations were calculated by normalizing peak areas to the elemental sensitivity factor data provided by the PHI database.

Results and Discussion

The synthetic procedure used for the $Cu/Cu_2O/CuO$ system serves to illustrate our development of a generalized method for the synthesis of transition metal oxide nanocrystals, which involves metal acetates as the precursors and thermal decomposition of metal acetate−surfactant complex in a hot organic

(15) Muramatsu, A.; Sugimoto, T. *J. Colloid. Interface Sci.* **1997**, *189*, 167.
(16) Ponyatovskil, E. G.; Arosimova, G. E.; Aronin, A. S.; Kulakov, V. I.; Sinitsyn, V. V. *Phys. Solid State* **2002**, *44*, 852.
(17) Mcfadyen, P.; Matijevic, E. *J. Colloid. Interface Sci.* **1973**, *44*, 95.
(18) Son, S. U.; Park, I. K.; Park, J.; Hyeon, T. *Chem. Commun.* **2004**, 778.
(19) Gou, L.; Murphy, C. J. *Nano Lett.* **2003**, *3*, 231.
(20) Ayyub, P.; Palkar, V. R.; Chattopadhyay, S.; Multani, M. *Phys. Rev. B* **1995**, *51*, 6135.
(21) Herhold, A. B.; Chen, C.-C.; Johnson, C. S.; Tolbert, S. H.; Alivisatos, A. P. *Phase Transitions* **1999**, *68*, 1.
(22) Qadri, S. B.; Skelton, E. F.; Hsu, D.; Dinsmore, A. D.; Yang, J.; Gray, H. F.; Ratna, B. R. *Phys. Rev. B* **1999**, *60*, 9191.
(23) Palkar, V. R.; Ayyub, P.; Chattopadhyay, S.; Multani, M. *Phys. Rev. B* **1996**, *53*, 2167.

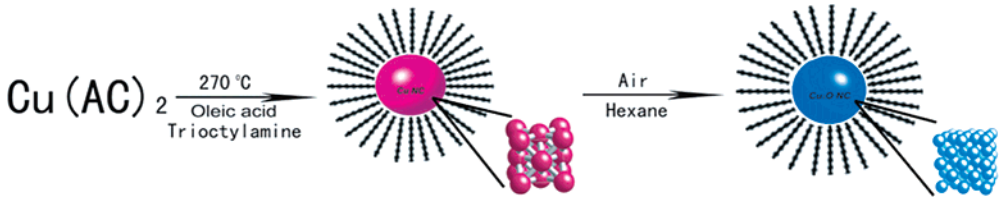

Figure 2. Synthetic procedure for Cu_2O nanocrystals.

solvent.[24,25] We have elected to call this method "TDMA" (thermal decomposition of metal acetates), and we believe it to be very effective for the synthesis of first-row transition metal and transition metal oxide nanocrystals (Figure 2).[26] Our method ensures the preparation of highly uniform, monodisperse nanocrystals of Cu_2O in high yield (typically >50−60% wrt conversion of precursor). Synthesis of transition metal oxide nanocrystals by choosing their acetates as precursors is simple and relatively safe.[24,25] Our experiments showed that, generally, the standard deviation of the size of nanocrystals prepared with solvent degassing (to remove O_2) is less than 5−10%, without further size selection. The as-synthesized nanocrystals have a capping coordination sphere of oleic acid, which stablilizes them in solution, prevents aggregation, and allows them to form close packed superlattice structures following evaporation of the solvent.

To obtain evidence that the nanoparticles formed in situ are initially pure copper nanocrystals, X-ray powder diffraction was performed immediately after sample preparation. There are a set of Bragg peaks in the XRD that could readily be indexed to the *fcc* structure of metal copper ($Fm\bar{3}m$, $a = 3.615$ Å, JCPDF no. 85-1326) (Figure 1a). The peaks are sharper than that of the final product (Figure 1b), indicating the presence of material larger than 5 nm; this was due to the rapid work up, which did not allow for more controlled precipitation from the reaction solvent. However, we believe the initial X-ray pattern, coupled with observed color changes during reaction, provides substantial evidence for a reaction mechanism that is based on reduction of the precursor to the pure transition metal with subsequent oxidation to the transition metal oxide. Only a very small peak of Cu_2O (110) was detected (and was also observed to grow slightly during XRD measurement), ascribed to nanocrystal oxidation *postsynthesis*. After controlled precipitation (separation of particles from any insoluble matter), the nanoparticles are dissolved in hexane and exposed to air. The color of the nanoparticle solution changes immediately to dark green, commensurate with oxidation to Cu_2O. XRD of this nanocrystal sample show that all of the peaks match well with Bragg reflections of the standard cubic cuprite structure ($Pn\bar{3}m$, $a =$ 4.267 Å, JCPDF no. 78-2076) as shown in Figure 1b. The process of full oxidation from Cu to Cu_2O nanocrystals can take up to a few hours, depending on the conditions and particle size; however, in all cases transformation to Cu_2O is complete, in contrast to previous reports.[18] The crystal structure of Cu_2O is cuprite, which is composed of eight cubes, as shown in Supporting Information Figure S3. In each cube, Cu atoms occupy all the *fcc* positions, and two oxygen atoms occupy two diagonal tetrahedral interstices. The oxidation can be qualitatively interpreted as an oxygen diffusion and lattice expansion process. As a result, the crystal structure and material changes from *fcc* Cu to cuprite Cu_2O with a corresponding lattice expansion (see Supporting Information, Figure S3). We note that Cu and Cu_2O share the high-symmetry cubic structure, while CuO is a low-symmetry monoclinic structure. There is a considerable energetic difference between the *fcc* structure (Cu) and monoclinic structure (CuO), as atom rearrangement and lattice/unit cell reconstruction is required, which may help to explain why the transformation to crystalline CuO does not occur in these nanocrystals, in addition to the possible stabilization of the (I) oxidation state by the ligand shell. Detailed structural analysis presented here reveals the presence of Cu^{2+} ions predominately at the surface, attributed to a thin layer of amorphous CuO which may also serve as kinetic stabilization with respect to further oxidation. Our results are consistent with other observations of Cu_2O stability at the nanoscale.[23]

Nanocrystal assembly from hexane solutions into closed packed arrays was also observed (Figure 3b), demonstrating the uniformity of the particle size and retention of the oleic acid capping group. Figure 3b shows a view of a close-packed superlattice of 6-nm Cu_2O nanocrystals. The nanocrystals are therefore presented as suitable candidates for the preparation of binary superlattice structures.[27] If the particle is oriented along a low-index zone axis, the distribution of atoms can be imaged. Figure 3c gives a profile HRTEM image of cubic Cu_2O nanocrystals. The lattice plane distance is 1.88 Å, indicating (210) planes. Selected area electron diffraction patterns (Figure 3d) can be indexed to cubic symmetry, confirming the cubic crystal structure of Cu_2O. Most nanocrystals (99%) are single crystal; however, twin structures of a single Cu_2O nanocrystal were also observed (Figure 4, occurring in this same form approximately in 1% of all nanocrystals). Twinning is one of the most popular planar defects in *fcc* structures.[28] Twinning is the result of two subgrains sharing a common crystallographic plane; thus, the structure of one subgrain is the mirror reflection of the other by the twin plane. The twin plane (Figure 4) is (111). It formed through rotation, either around the ⟨111⟩ or ⟨112⟩ axis. Generally, twinning can be a result of deformation and/or dislocation motions in a cubic system. In our case, we believe twinning is sometimes induced due to the volume change of the two phases when Cu transforms to Cu_2O.

The role of the capping ligand is very important to nanocrystal synthesis, during nucleation, growth, and stabilization of the particles, and also important to postsynthesis, with respect to agglomeration and stabilization in organic solvents. We observed a decrease of particle size from 10.7 ± 0.7 to 3.6 ± 0.8 nm as the molar ratio of copper (I) acetate to oleic acid was increased

(24) Yin, M.; Gu, Y.; Kuskovsky, I. L.; Andelman, T.; Zhu, Y.; Neumark, G. F.; O'Brien, S. *J. Am. Chem. Soc.* **2004**, *126*, 6206.
(25) Yin, M.; O'Brien, S. *J. Am. Chem. Soc.* **2003**, *125*, 10180.
(26) Park, J.; An, K.; Hwang, Y.; Park, J.-G.; Noh, H.-J.; Kim, J. Y.; Park, J.-H.; Hwang, N.-M.; Hyeon, T. *Nat. Mater.* **2004**, *3*, 891.
(27) Redl, F. X.; Cho, K.-S.; Murray, C. B.; O'Brien, S. *Nature* **2003**, *423*, 968.
(28) Wang, Z. L. *J. Phys. Chem. B.* **2000**, *104*, 1153.

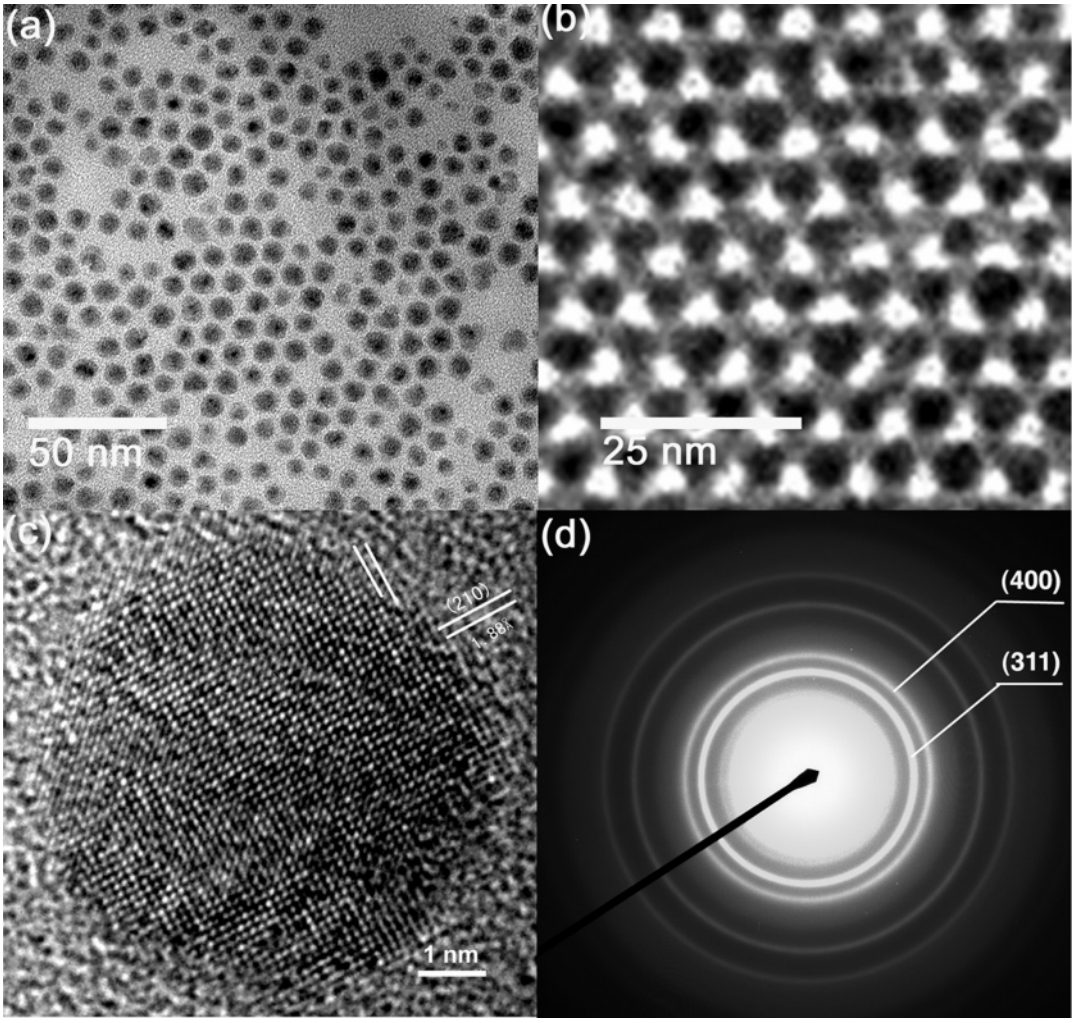

Figure 3. (a) Transmission electron micrograph (TEM) of self-assembled 6-nm diameter Cu_2O nanocrystals. (b) TEM image showing a larger area view of a close-packed superlattice of 6-nm Cu_2O nanocrystals. (c) High-resolution image showing the single crystal and high crystallinity. (d) Selected area electron diffraction pattern of Cu_2O nancrystals.

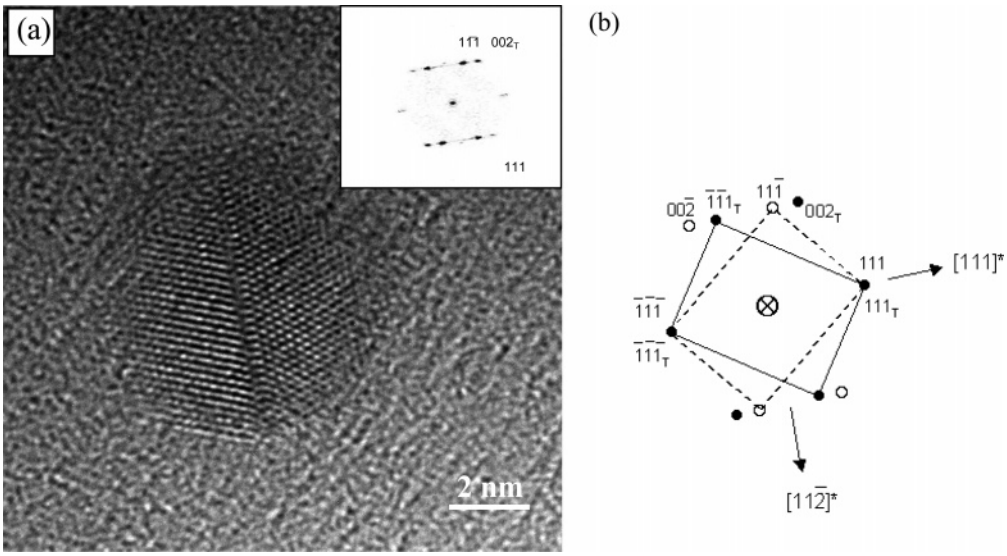

Figure 4. (a) HRTEM image showing a twin structure in a single Cu_2O nanocrystal. (Insert) Corresponding FFT. (b) Schematic of twinning orientation.

from 0.08 to 0.6 (Supporting Information, Figure S2). The ability to control particle size is of fundamental interest to prepare high-quality, monodisperse cuprous oxide nanocrystals and to characterize their optical properties.

Understanding size effects in such a system provides the possibility of tuning its optoelectronic properties for specific applications. The absorption spectrum of Cu_2O nanocrystals (Figure 5) shows two hump-like optical absorption features at

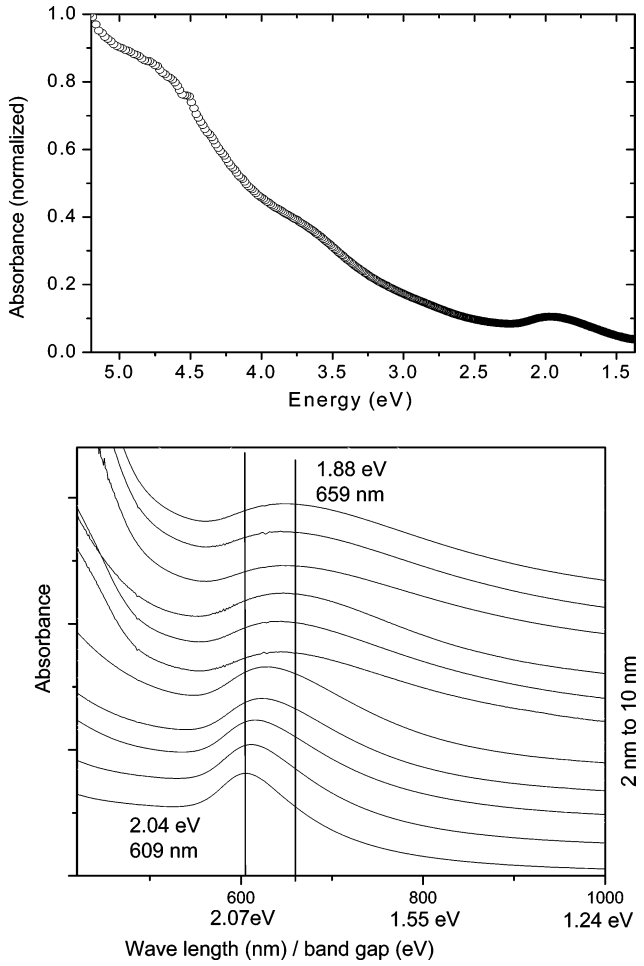

Figure 5. (a) UV−vis spectrum of as-prepared 6-nm Cu_2O nanocrystals in hexane at 298 K (b) UV−vis spectra of Cu_2O nanocrystals size selected over the 2−10-nm range.

about 260 and 340 nm, which are attributed to band-to-band transition in the nanocrystalline Cu_2O.[7,29] Another weak, broad feature centered at 630 nm is also observed, which is attributed to the band gap transition of CuO, present at the surface of the nanocrystal.[7] We conclude that such a layer of CuO exists and provides further compelling quantitative evidence by XPS. The band gap energy of bulk CuO is 1.2−1.5 eV.[30−32] The blue-shift of 0.5−0.8 eV of the CuO band gap absorption might be the result of quantum confinement. The absorption is assigned to the thin layer of CuO, but it remains unknown whether this layer is amorphous or crystalline, and we consider it a monolayer shell of continuous CuO. There is no observable emission spectrum for the as-synthesized Cu_2O nanocrystals. The exciton states in Cu_2O consist of the spin singlet Γ_2 "paraexciton" and the spin triplet Γ_{12} "orthoexciton". Direct recombination for the paraexciton is dipole- and quadrupole forbidden, while the orthoexciton is dipole forbidden because of the inversion symmetry of the crystal. Therefore, the primary luminescence mechanism is phonon-assisted recombination of exciton, which

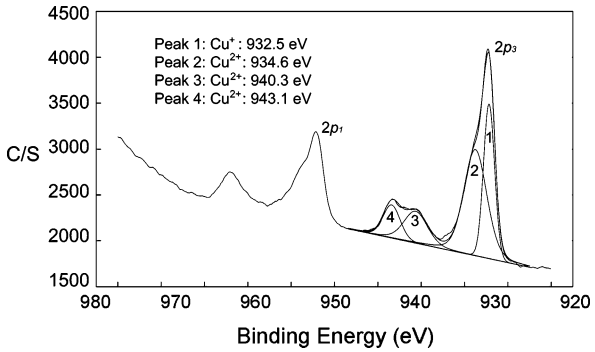

Figure 6. X-ray photoelectron spectrum of 6-nm Cu2O nanocrystals, showing Cu $2p_{3/2}$ and Cu $2p_{1/2}$ at 932.5 eV and 952.7 eV, respectively. The peakfit of Cu $2p_{3/2}$ peak revealed a main peak at 932.5 eV and accompanied by a series of satellites on the high-binding-energy side, 934.6, 940.3, and 943.1 eV respectively.

is at least a factor of 30 weaker, consistent with the profile of the spectrum.[33]

In the interests of investigating the optical properties of the nanocrystals as a function of size, we collected Cu_2O nanocrystal samples after the decomposition at 0 (less than 1), 1, 2, 3, 5,-10, 20, 30, 45, 60 and 120 min, respectively, and took the UV−vis spectra (Figure 5b). TEM analysis of the samples at the earlier times showed size distributions progressing from nanoparticle diameters of ∼2−8 nm, while the average particle diameter at 20, 30, 45, 60 and 120 min was found to be 8.5, 8.9, 9.7, 10.0, and 9.8 nm, respectively. The broad feature centered at 630 nm in 6-nm nanocrystals, attributed to the band gap transition of the surface CuO layer, can be observed to be highly blue-shifted at the smaller-size diameters (centered at 2.07 eV). The blue-shift progressively decreases with increasing particle diameter (moving to 1.88 eV), providing further evidence for a possible quantum confinement effect. X-ray photoelectron spectroscopy of 6-nm particles provided evidence that the CuO layer is ∼0.5 nm thick (outlined in detail below). The CuO unit cell has typical dimensions, $a = 4.6873$ Å, $b = 3.4226$ Å, $c = 5.1288$ Å,[30] suggesting the CuO layer appears to be essentially a unit cell monolayer, too thin to be detected by X-ray powder diffraction. We believe that this uniquely thin CuO layer gives rise to the presence of a shifting peak (2.07 to 1.88 eV) as a function of nanocrystal diameter (from 2 to 10 nm) in the absorption profile observed in the UV−vis spectrum.[7,29]

The evidence in the optical profile of the presence of a CuO on the Cu_2O nanocrystals in the present study warranted in-depth investigation by X-ray photoelectron spectroscopic measurements (Figure 6). XPS is a powerful technique for the study of transition metal compounds having localized valence d orbitals. In CuO, copper exists in the divalent state having mainly d^9 character. However, Cu_2O is expected to have an essentially full Cu 3d shell.[30] The XPS detected the Cu $2p_{3/2}$ and Cu $2p_{1/2}$ at 932.5 and 952.7 eV respectively. The peak-fit of Cu $2p_{3/2}$ peak revealed a main peak at 932.5 eV and was accompanied by a series of satellites on the high-binding-energy side, 934.6, 940.3, and 943.1 eV, respectively. The main peak was known as characteristics of Cu^+ and the shake-up satellite peaks are evident and diagnostic of an open $3d^9$ shell, corre-

(29) Pestryakov, A. N.; Petranovskii, V. P.; Kryazhov, A.; Ozhereliev, O.; Pfander, N.; Knop-Gericke, A. *Chem. Phys. Lett.* **2004**, *385*, 173.
(30) Ghijsen, J.; Tjeng, L. H.; Elp, J. v.; Eskes, H.; Westerink, J.; Sawatzky, G. A. *Phys. Rev. B* **1988**, *38*, 11322.
(31) Ito, T.; Yamaguchi, H.; Masumi, T.; Aldachi, S. *J. Phys. Soc. Jpn.* **1998**, *67*, 3304.
(32) Koffyberg, F. P.; Benko, F. A. *J. Appl. Phys.* **1982**, *53*, 1173.
(33) Snoke, D. W.; Shields, A. J.; Cardona, M. *Phys. Rev. B* **1992**, *45*, 11693.

sponding to Cu^{2+} state.[30,34] The relative intensities of the shake-up satellites from these levels are indicative of the presence of CuO at the surface.[35] The fact that XRD does not show evidence of CuO phase, while XPS indicates the surface presence of Cu^{2+} ions, suggests that CuO is present only on the surface of the Cu_2O nancrystals and it forms a thin amorphous outer shell. By basing the XPS data on a core−shell model of Cu_2O/CuO, it is possible to estimate the thickness of the CuO layer, which we found to be about ∼5 Å for an average diameter of 6 nm. Details of this calculation are presented in the Supporting Information.

In summary, monodisperse, stable Cu_2O nanocrystals were synthesized by using a novel, yet simple wet chemistry route. This reliable method gives a high yield of nanocrystals and narrow size distributions. The Cu_2O nanocrystal diameter could be tuned from 3.6 to 10.7 nm by controlling the molar ratio of oleic acid to copper precursor. From structural analysis we conclude that the Cu_2O phase is highly stabilized in these nanocrystals. The investigated nanocrystals displayed a band gap transition attributed to the presence of a CuO monolayer shell (too thin to be detected by XRD), the transition was observed to shift toward the blue as a function of decreasing particle size. X-ray photoelectron spectroscopy determined that the CuO monolayer shell was approximately 5 Å in 6-nm Cu_2O nanocrystals. The nanocrystals could be assembled into 3D superlattices and are presented as candidates for multicomponent assembly.

Acknowledgment. This work was supported primarily by the U.S. Department of Energy, Office of Basic Energy Sciences, through the Catalysis Futures Grant DE-FG02-03ER15463, in part by the MRSEC Program of the National Science Foundation under award number DMR-0213574, and O'Brien's NSF-CAREER award, DMR-0348938.

Supporting Information Available: Additional figures and calculations. This material is available free of charge via the Internet at http://pubs.acs.org.

JA050006U

(34) Chawla, S. K.; Sankarraman, N.; Payer, J. H. *J. Elec. Spectrosc. Relat. Phenom.* **1992**, *61*, 1.
(35) Chusuei, C. C.; Brookshier, M. A.; Goodman, D. W. *Langmuir* **1999**, *15*, 2806.